



## Synthesis of zeolite membrane (MCM-22/ $\alpha$ -alumina) and its application in the process of oil-water separation

Antonielly S. Barbosa\*, Antusia S. Barbosa, Meiry G.F. Rodrigues

Academic Unit of Chemical Engineering, Federal University of Campina Grande, Av. Aprígio Veloso, 882 – Bodocongó, CEP 58109 970, Campina Grande, Brazil, Tel. +55 83 2101 1488; emails: [antoniellybarbosa@yahoo.com.br](mailto:antoniellybarbosa@yahoo.com.br) (Antonielly S. Barbosa), [antusiasb@hotmail.com](mailto:antusiasb@hotmail.com) (Antusia S. Barbosa), [meirygfr@hotmail.com](mailto:meirygfr@hotmail.com) (M.G.F. Rodrigues)

Received 15 July 2014; Accepted 26 November 2014

### ABSTRACT

Zeolite membrane (MCM-22/ $\alpha$ -Al<sub>2</sub>O<sub>3</sub>) was prepared on  $\alpha$ -Al<sub>2</sub>O<sub>3</sub> disk by synthesis method (rubbing) and investigated through water separation and oily water recovery. The materials were characterized by X-ray diffraction (XRD), scanning electron microscopy (SEM), and mercury porosimetry. Thereafter, the separation of oil-water emulsion was evaluated. The crystallization behavior of the particles of the zeolite membrane is observed through the XRD. The images obtained by SEM of the zeolite membrane (MCM-22/ $\alpha$ -Al<sub>2</sub>O<sub>3</sub>) showed that the method used for the synthesis of the zeolite membrane was effective since it showed the formation of a homogeneous surface with no cracks or defects on the surface of the porous support of  $\alpha$ -Al<sub>2</sub>O<sub>3</sub>. Oil rejection was monitored. Fouling occurred as a layer on the membrane surface. The test showed that the MCM-22 zeolite membrane has potential for oil-water separation.

*Keywords:* MCM-22 zeolite membrane; Rubbing;  $\alpha$ -Al<sub>2</sub>O<sub>3</sub>; Oil-water

### 1. Introduction

Oily wastewater from industry and domestic sewage is one of the main pollutants to the environment in the world. With the production of crude oil and natural gas, an aqueous stream named “produced water” is normally accompanied due to the hydraulic fracturing process. The produced water, which contains dispersed oils, suspended particles, and dissolved solutes, constitutes the largest waste stream made of oil and gas of manufacturing industries [1].

Industrialization and urbanization have accelerated water pollution; consequently, water has become a limited resource. Recycled wastewater can reduce environmental damage and it can be an alternative water source which can reduce the demands for fresh water [2].

Oil-in-water (o-w) or water-in-oil (w-o) emulsions can be generated from various industrial processes, such as metallurgical process, transportation, food processing, and petrochemical process, as well as, petroleum refineries. Typical composition ranges of “produced water” generated from oil and gas industrial processes include 50–1,000 mg/L of total oil and

\*Corresponding author.

Presented at the IX Ibero-American Congress on Membrane Science and Technology (CITEM 2014), 25–28 May 2014, Santander, Spain

grease and 50–350 mg/L of total suspended solids. Environmental regulations require that maximum total oil and grease concentration in discharge waters are 15 mg/L [3].

The removal of oil from oil-in-water emulsion is an important aspect of pollution control [4].

In order to establish environmental standards, as well as, the reuse and the recycling of produced water, many researchers have focused on treatment of oily saline produced water [5].

The treatment of the oil-water emulsion, in which the droplets of micron or submicron size uniformly disperse in large amounts of water in the surfactant stabilized oil, was considered ineffective by conventional gravity separation, skimming, air flotation, coagulation, and flocculation, among other methods [4].

As a result, the physical separation membrane processes based on microarrays made for the twenty-first century pressure-driven membrane processes depend on the pore size of the membrane to separate feed stream components according to their pore sizes [5].

The membrane can be described as a semi-permeable barrier between two phases that prevents intimate contact. The barrier must be permselective [6].

Many studies have been developed on the different treatments of oily membranes with effluents. Ceramic membranes have been known for years, and used in many different applications, due to their numerous advantages: Stability at high temperature and pressure resistance, good chemical stability, high mechanical strength, good durability, and anti-fouling properties. Ceramic MF membrane can be made of alumina, mullite, cordierite, silica, spinel, zirconia, and other refractory oxides [3].

Microfiltration membranes used in the treatment of oily wastewater often have pore sizes of 0.2–0.8 nm prepared by any of the sintering methods of the particles, or by a sol–gel process [7].

A significant disadvantage of membrane purification is membrane fouling, which can happen due to several factors, such as adsorption within the membrane, and deposition on the membrane surface to block the membrane pores [8].

Generally, surface modification is used to improve the performance of membrane anti-fouling, such as masking the outer surfaces of the membranes with hydrophilic polymers. Recently, hydrophobic surfaces with wettability and superoleophilic properties have attracted great interest in the filtration field. They differ from the traditional membranes used for the oil and water separation [9].

Zeolite membranes have stable chemical, mechanical, thermal, and anti-fouling properties. They can be used in mediums of strong solvents and high

temperatures and pressures. RO zeolite membranes are suitable for the treatment of oilfield-produced water to separate different ions ( $\text{Na}^+$ ,  $\text{K}^+$ ,  $\text{Ca}^{2+}$ , and  $\text{Mg}^{2+}$ ) [5].

Zeolite membranes are formed by intergrown zeolite particles with interparticle pores filled with another material. The intracrystalline pores are part of the crystallographic structure and have a very uniform diameter [6].

In recent decades, intensive research has been developed about the synthesis of zeolite membranes by catalytic membrane reactors, taking advantage of its attractive molecular sieve and the catalytic properties [10].

For a better performance in separation, zeolite membranes are preferably formed of zeolite crystals with uniform size and small particles. Several preparation methods have been developed, such as *in situ* hydrothermal synthesis, vapor-phase transport method, and secondary growth method [11].

In this article, a disk-shaped zeolite membrane with hydrophobic surface (zeolite) was made by secondary growth method. The aim of this work is the use of thin hydrophobic porous membranes for the separation of suspensions of oil-in-water emulsion.

## 2. Experimental

### 2.1. Materials

Alumina, sodium aluminate (50–56%  $\text{Al}_2\text{O}_3$ , maximum 0.05%  $\text{Fe}_2\text{O}_3$ , 40–45%  $\text{Na}_2\text{O}$ , Riedel-deHaen), sodium hydroxide (NaOH—97%, Merck), deionized water, silica aerosil ( $\text{SiO}_2$ —Aerosil 200, Degussa), hexamethyleneimine (HMI 99%, Aldrich), oleic acid, PABA (para-aminobenzoic acid), and ethyl alcohol (Vetec, P. A. ACS (ethanol)  $\text{C}_2\text{H}_6\text{O}$ ).

### 2.2. Preparation of the samples

#### 2.2.1. Ceramic membrane preparation ( $\alpha\text{-Al}_2\text{O}_3$ )

Calcined alumina A1000 SG (ALMATIS, Inc.) was used for the synthesis of ceramic ( $\alpha\text{-Al}_2\text{O}_3$ ) membrane. Two hundred milliliters of dispersion with the following composition was prepared, which includes 40% alumina; PABA 0.2% para-amino benzoic acid (dissolved in ethanol); 0.5% oleic acid (lubricant); and 59.3% ethyl alcohol. The mixture was ground for 1 h in a ball mill and then placed in an oven for 24 h at 60°C; humidify itself with 7% water, resting for one day. Three grams of the material was weighed and placed in the mold. The pressing was performed with 4 ton. The compressed material was submitted to sintering at 1,200°C for 1 h [12].

### 2.2.2. Zeolite MCM-22 preparation

The samples were prepared by a synthetic method described elsewhere [13]. The hydrothermal synthesis of the layered aluminosilicate MCM-22 was carried out using hexamethyleneimine as an organic template at dynamic conditions. A total of 3.110 g of anhydrous sodium aluminate (50–56%  $\text{Al}_2\text{O}_3$ , maximum 0.05%  $\text{Fe}_2\text{O}_3$ , 40–45%  $\text{Na}_2\text{O}$ , purchased from Riedel-deHaën) and 1.930 g of sodium hydroxide (97%, from Merck) were dissolved in 415 g of deionized water. The solution was thoroughly stirred for 15 min, after which 25.4 g of hexamethyleneimine (HMI) (99%, from Aldrich) was added dropwise while stirring vigorously. Then, 30.7 g of silica (Aerosil 200, Degussa) was added in small portions to the mixture being stirred and the resulting slurry continued to be stirred vigorously. After 30 min of stirring, at room temperature, a gel was formed and then placed in an autoclave, and heated at 150 °C for 10 d. After immersing the autoclaves in cold water, the resulting material was washed and centrifuged up to  $\text{pH} \leq 9$ , and subsequently dried at 60 °C.

### 2.2.3. Zeolite membrane preparation (MCM-22/ $\alpha$ - $\text{Al}_2\text{O}_3$ )

The MCM-22 zeolite membrane was prepared using the secondary growth (rubbing) technique.

The crystals deposited on the ceramic ( $\alpha$ - $\text{Al}_2\text{O}_3$ ) support were then carefully rubbed manually. The procedure is similar to Ref. [14].

This support was submitted to a secondary growth technique. The synthesis condition was the same as that of the *in situ* growth. After the crystallization, the membrane was washed thoroughly with water. Then, the membrane was dried at 60 °C for 24 h.

### 2.3. Characterization of the samples

**X-ray diffraction (XRD):** The powder method was used, in which the samples were sieved in an ABNT n. 200 (0.074 mm) sieve and then placed in an aluminum specimen holder for XRD, using a Shimadzu XRD 6000 equipment. Operational details of the technique have been set as follows: Copper  $K\alpha$  radiation at 40 kV/30 mA, with a goniometer velocity of  $2^\circ \text{min}^{-1}$  and a step of  $0.02^\circ$  in the range of  $2\theta$  scanning from  $2^\circ$  to  $45^\circ$ . The only d-spacing of interest in the X-ray patterns was the basal spacing along the *c* axis.

**Scanning electron microscopy (SEM):** The powder samples were recovered with a thin layer of gold, due to the high electron conductivity of this metal, fixed in

the alumina specimen holder by an adhesive carbon tape. The micrographics needed to analyze the morphology of the samples which were obtained through a scanning electron microscope Philips XL 30 EDAX, equipped with X-ray energy dispersion spectrophotometer.

**Mercury porosimetry:** It was performed on a mercury porosimeter, model Autopore IV 9500 V1.05.

### 2.4. Treatment of oil-in-water emulsion

Oily wastewater was prepared emulsifying 0.05 g of lubricant oil (LUBRAX) in 500 mL of distilled water under stirring (high-speed stirrer) for 20 min to produce stable emulsion.

The membrane filtration was carried out at a pressure of 1 bar for ceramic membrane ( $\alpha$ - $\text{Al}_2\text{O}_3$ ) and for the MCM-22 zeolite membranes. The oil concentrations of the feed and permeate streams were analyzed.

The concentration of oil present in the aqueous phase was determined by analysis of absorbance using a UV–visible spectrophotometer. Initially, a calibration curve of absorbance vs. concentration was constructed using previously defined concentrations of oil. These concentrations ranged from 0 to 100 ppm and the solvent used for extraction was chloroform, showing a response (significant peak) at a wavelength of 262 nm for the analyzed samples. The absorbance at this wavelength is commonly used to estimate the concentration of oil in water samples and also in produced water. Bands of aromatic CH in the medium are measured at this wavelength. Based on this, the absorbance was measured at this wavelength. This implementation procedure was designed to normalize the determination of oil and grease contents [15].

The permeate flow was calculated by dividing the permeate volume by the product of the membrane area and the sampling time, and the oil rejection coefficient *R* was calculated as a percentage according to the following expression:

$$\%R = \left( \frac{C_f - C_p}{C_f} \right) \times 100$$

where  $C_f$  is the oil concentration in the feed, and  $C_p$  is the oil concentration in the permeate.

## 3. Results and discussion

The results of XRD of samples of MCM-22 zeolite, ceramic membrane, and MCM-22 zeolite membrane are shown in Fig. 1.

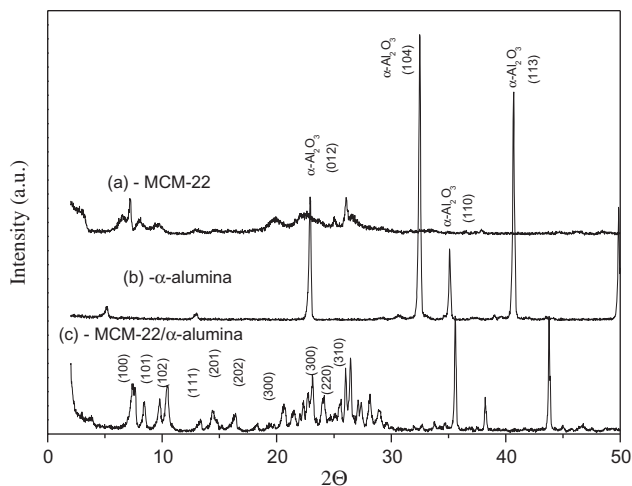


Fig. 1. XRD patterns of the samples: MCM-22 zeolite, ceramic membrane ( $\alpha$ - $\text{Al}_2\text{O}_3$ ), and zeolite membrane (MCM-22/ $\alpha$ - $\text{Al}_2\text{O}_3$ ).

Two distinct phases can be identified as a constituent of the zeolitic membrane structure: MCM-22 zeolite and clay ( $\alpha$ - $\text{Al}_2\text{O}_3$ ) membranes are shown in Fig. 1(c). The XRD pattern showed that the MCM-22 zeolite synthesized on the ceramic membrane ( $\alpha$ -alumina) showed crystalline structure as described by Yang et al. [16] without evidence of other crystalline phases (impurities). The formation of MCM-22 zeolite on the surface of the porous ( $\alpha$ - $\text{Al}_2\text{O}_3$ ) membrane can be confirmed by observation of characteristic peaks in the regions corresponding to  $2\theta = 12$ – $25^\circ$  and  $2\theta = 26$ – $29^\circ$ ; the peaks have good intensity [13].

In Fig. 2, SEM image of the samples:  $\alpha$ - $\text{Al}_2\text{O}_3$  and zeolite membrane (MCM-22/ $\alpha$ - $\text{Al}_2\text{O}_3$ ) are shown.

Fig. 2(b) provides an example of a MCM-22 zeolite membrane. Two different morphologies were observed in the zeolite MCM-22 membrane. After a detailed examination of the cross section (Fig. 2(c)), the membrane showed a layer composed of crystals of zeolite MCM-22 materials synthesized under the surface of the ceramic membrane ( $\alpha$ - $\text{Al}_2\text{O}_3$ ) (Fig. 2(a)), the image displayed by this layer is in accordance with the ceramic membrane ( $\alpha$ - $\text{Al}_2\text{O}_3$ ) [17].

The morphology of the active layer (MCM-22 zeolite) formed on the surface of the ceramic ( $\alpha$ - $\text{Al}_2\text{O}_3$ ) with membrane showed spherical crystals. This behavior was also observed by Barbosa et al. [18].

The graphic of average pore diameter, as a function of cumulative intrusion volume of mercury in the ceramic membrane ( $\alpha$ - $\text{Al}_2\text{O}_3$ ), is shown in Fig. 3.

It is observed that the ceramic membrane ( $\alpha$ - $\text{Al}_2\text{O}_3$ ) shows most of the pore diameters between 2.0 and 0.4  $\mu\text{m}$ , as it can be observed in the curve slope.

Fig. 4 shows the graphic of the distribution of average pore diameters of the ceramic membrane ( $\alpha$ - $\text{Al}_2\text{O}_3$ ).

It was verified that the unimodal ceramic membrane ( $\alpha$ - $\text{Al}_2\text{O}_3$ ) has a structure and narrow pore size distribution; this is the factor that is characterized as highly selective in the region from 2.0 to 0.4  $\mu\text{m}$ .

The values of average pore diameter and the porosity of the ceramic ( $\alpha$ - $\text{Al}_2\text{O}_3$ ) membrane support are shown in Table 1.

According to the average pore diameter, the ceramic membrane ( $\alpha$ - $\text{Al}_2\text{O}_3$ ) can be classified as microfiltration membranes, such as Ref. [19]. And, because of its narrow range of pore size distribution, it is very likely that the membrane has high selectivity.

The variation of pore diameter of the zeolite membrane according to the intrusion volume of mercury accumulated in the MCM-22 zeolite membrane is presented in Fig. 5.

From Fig. 5, it can be seen that the zeolitic membrane (MCM-22/ $\alpha$ - $\text{Al}_2\text{O}_3$ ) has the largest pore diameter which varies around 0.76–0.16  $\mu\text{m}$ . The value found for the pore diameter of the zeolitic membrane (MCM-22/ $\alpha$ - $\text{Al}_2\text{O}_3$ ) was similar to that for the value of ceramic membrane ( $\alpha$ - $\text{Al}_2\text{O}_3$ ).

The graphic of the distribution of average pore diameters of the (MCM-22/ $\alpha$ - $\text{Al}_2\text{O}_3$ ) zeolite membrane is present in Fig. 6 and the average pore diameter and its porosity are shown in Table 2.

According to Fig. 6, there was a unimodal behavior for the zeolite membrane (MCM-22/ $\alpha$ - $\text{Al}_2\text{O}_3$ ) and a narrow pore size distribution in the region of 0.76–0.16  $\mu\text{m}$ .

According to Table 2, the MCM-22 zeolite membrane had an average pore diameter in the microfiltration range, about 0.61  $\mu\text{m}$  [20].

### 3.1. Zeolite membrane treatment of oil-in-water emulsions

Fig. 7 shows the curve of the measured flow in water/oil emulsion in a cell for the filtration ceramic membrane ( $\alpha$ - $\text{Al}_2\text{O}_3$ ) to MCM-22 zeolite membrane.

Fig. 7 shows the flow measurements for the ceramic membrane ( $\alpha$ - $\text{Al}_2\text{O}_3$ ) and MCM-22 zeolite membrane. The flow of permeate through the ceramic membrane and the zeolite membrane was stable throughout the time interval. The microfiltration membranes show similar behavior to that shown in Fig. 7 [21,22].

Fig. 8 shows the measures (rejection coefficient) vs. time obtained using water-oil emulsion for the ceramic membrane ( $\alpha$ - $\text{Al}_2\text{O}_3$ ) to MCM-22 zeolite membrane.

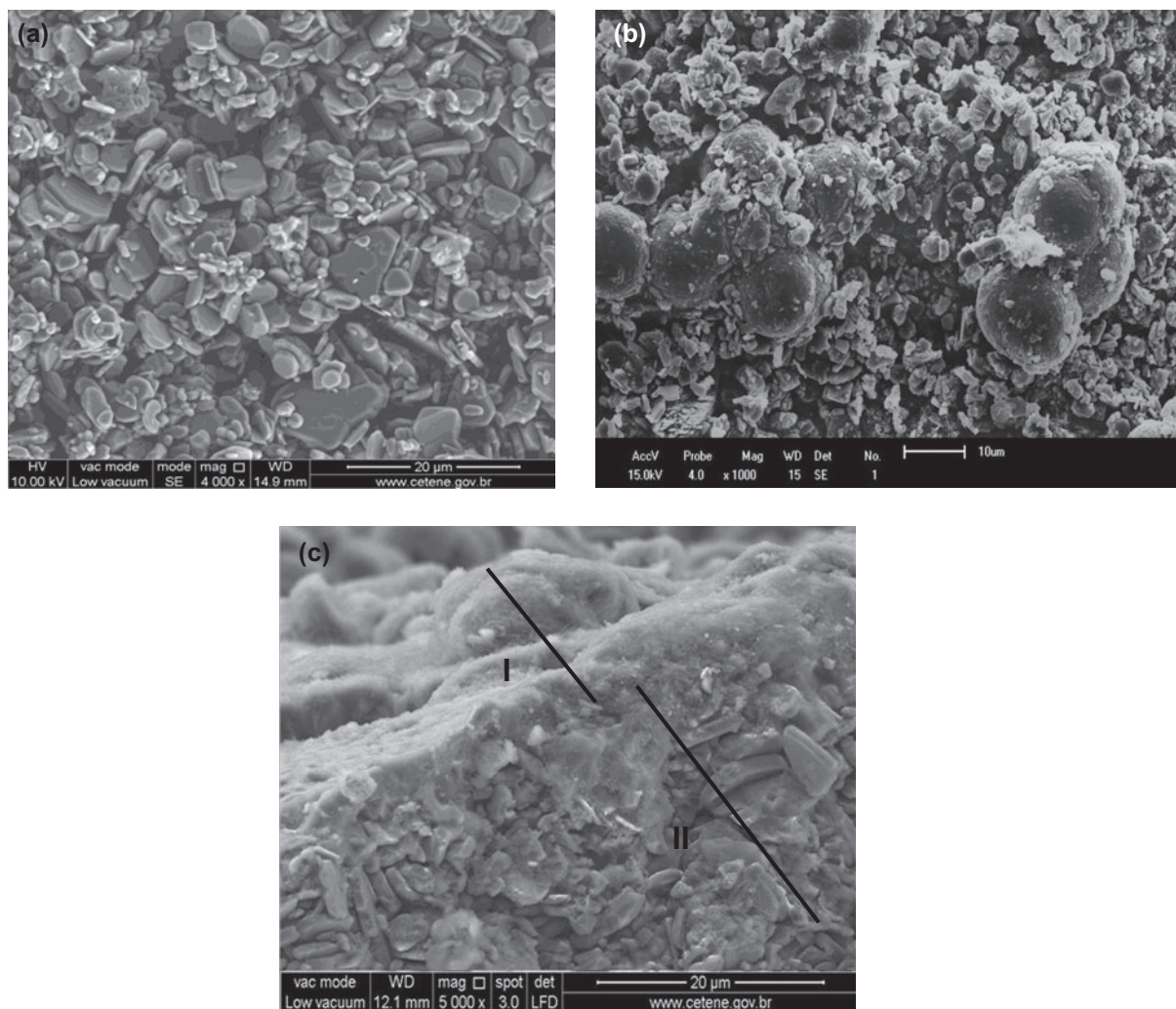


Fig. 2. SEM images of the samples: (a) Ceramic membrane  $\alpha\text{-Al}_2\text{O}_3$ , (b) zeolite membrane (MCM-22/ $\alpha\text{-Al}_2\text{O}_3$ ), and (c) cross-sectional view of the MCM-22 zeolite membrane.

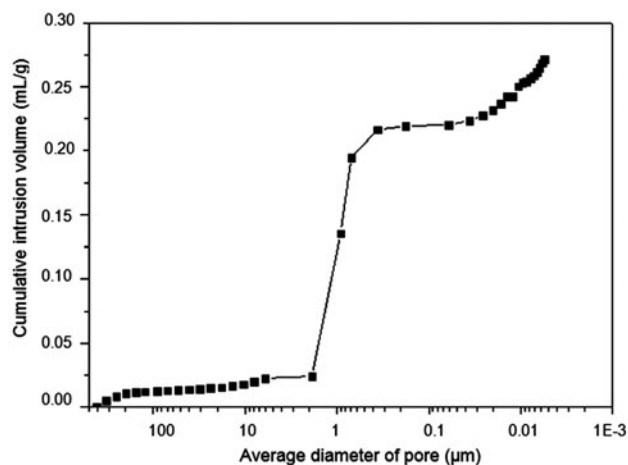


Fig. 3. Graphic of average pore diameter of cumulative intrusion volume of mercury in the ceramic membrane ( $\alpha\text{-Al}_2\text{O}_3$ ).

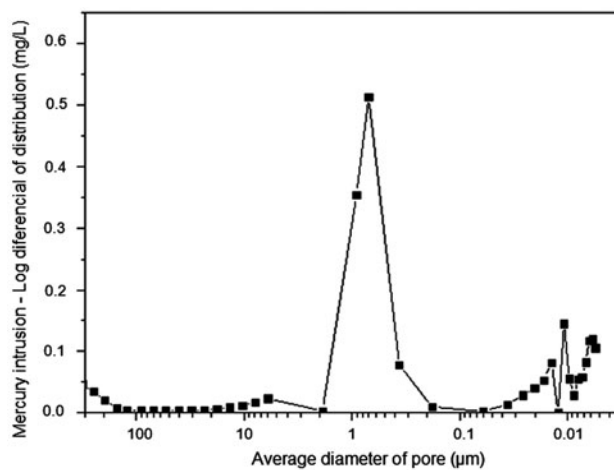


Fig. 4. Graphic of the distribution of average pore size due to the variation in the intrusion volume of mercury in ceramic membrane ( $\alpha\text{-Al}_2\text{O}_3$ ).

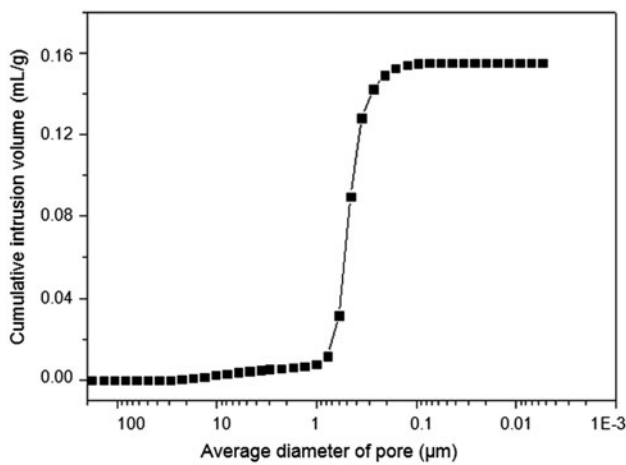


Fig. 5. Graphic of average pore diameter of cumulative intrusion volume of mercury in the zeolite membrane MCM-22.

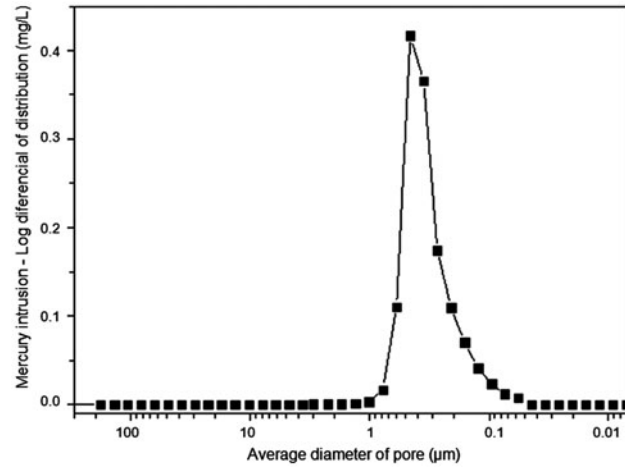


Fig. 6. Graphic of the distribution of average pore size due to the variation in the volume of mercury intrusion in the zeolite membrane MCM-22.

Table 1

Values of average pore diameter and the porosity of the ceramic membrane ( $\alpha$ -Al<sub>2</sub>O<sub>3</sub>)

	Average pore diameter ( $\mu\text{m}$ )	Porosity (%)
Ceramic membrane ( $\alpha$ -Al <sub>2</sub> O <sub>3</sub> )	0.71	33.37

Table 2

Values of average pore diameter and the porosity of the zeolite membrane (MCM-22/ $\alpha$ -Al<sub>2</sub>O<sub>3</sub>)

	Average pore diameter ( $\mu\text{m}$ )	Porosity (%)
Zeolite membrane (MCM-22/ $\alpha$ -Al <sub>2</sub> O <sub>3</sub> )	0.61	36.75

According to Fig. 8, the values obtained for zeolite membrane MCM-22 vary between 60 and 100%. In general, it can be noted that the increase in concentration of oil on the surface of the membranes resulted in a greater efficiency in all membranes.

The ceramic membrane ( $\alpha$ -Al<sub>2</sub>O<sub>3</sub>) and MCM-22 zeolite membrane were used in the separation process of oil-water emulsions; the oil droplets of the emulsion varied between 4.90 and 5.63  $\mu\text{m}$  in diameter.

Fig. 9 shows the oil concentration in permeate stream as a function of time for the  $\alpha$ -Al<sub>2</sub>O<sub>3</sub> disk and zeolite membrane (MCM-22/ $\alpha$ -Al<sub>2</sub>O<sub>3</sub>).

After detailed examination, the flow measurements of the oil content in the permeate product, in Fig. 9, it can be seen that, in the beginning of the process, the MCM-22 zeolite membrane obtained a higher percentage of oil removal in comparison to ceramic

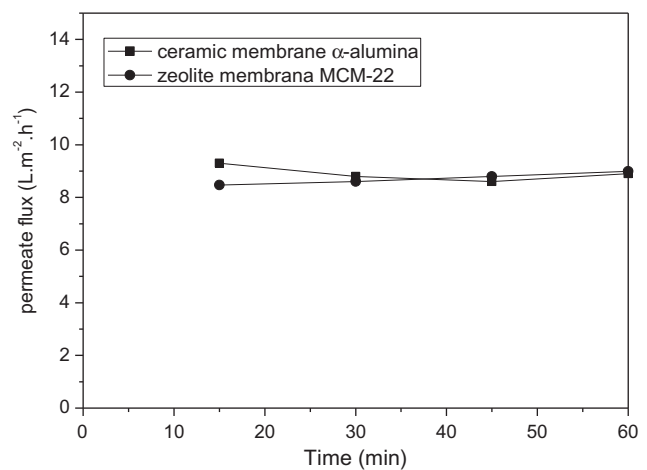


Fig. 7. Graphic of (a) ceramic membrane ( $\alpha$ -Al<sub>2</sub>O<sub>3</sub>) and (b) MCM-22 zeolite membrane.

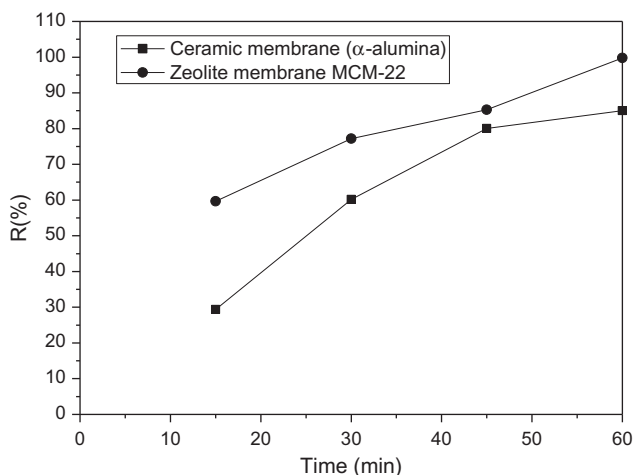


Fig. 8. Graphics of oil rejection coefficient of (a) ceramic membrane ( $\alpha$ -Al<sub>2</sub>O<sub>3</sub>) and (b) MCM-22 zeolite membrane.

membrane ( $\alpha$ -Al<sub>2</sub>O<sub>3</sub>). This fact can be explained due to the MCM-22 zeolite layer deposited on the surface of ceramics ( $\alpha$ -Al<sub>2</sub>O<sub>3</sub>) membrane, which increases the efficiency of the separation process.

From Fig. 9, it can be observed that the MCM-22 zeolite membrane showed removal percentages equivalent to the standards required by Resolution 392 of Ref. [23].

It seems that after 40 min of monitoring the system, the removal of oil from the oil-water emulsion is greater. This can be attributed to the fact that the oil concentration on the surface of the filtering medium causes a clogging in the membrane, with a likely

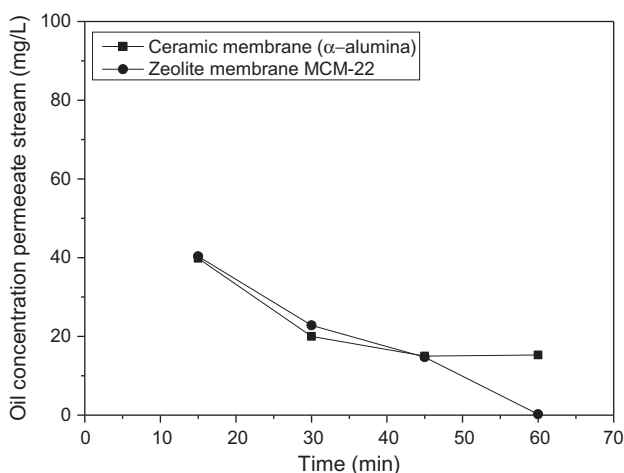


Fig. 9. Graphic of oil concentration in permeate stream of ceramic ( $\alpha$ -Al<sub>2</sub>O<sub>3</sub>) membrane and zeolite membrane (MCM-22/ $\alpha$ -Al<sub>2</sub>O<sub>3</sub>).

polarization of concentration near the surface of the membrane.

In general, it was observed that the oil concentration on the surface of the membranes resulted in a greater efficiency for both the ceramic membrane ( $\alpha$ -alumina) and for zeolite MCM-22 membrane. This fact can be attributed to the formation of an oil layer on the surface of the membranes leading to clogging, obstructing the passage of the same through the membrane.

#### 4. Conclusions

The XRD pattern showed that the MCM-22 zeolite membrane obtained by the secondary growth method—rubbing, synthesized on the ceramic membrane crystalline structure, showed no evidence of other phases characterized as impurities. SEM images of the MCM-22 zeolite membrane showed the formation of a zeolite layer over the ceramic membrane, which spherical particles grown on the surface of the ceramic membrane. The MCM-22 zeolite membrane in this separation process of oil-water emulsions achieved a significant reduction of oil concentration in the permeate showing, thereby, that it has the potential for this application.

#### Acknowledgments

The authors thank Petrobras for financial support and to improve (Coordenação de Aperfeiçoamento de Pessoal de Nível Superior) (CAPES) for the scholarship granted.

#### References

- [1] S. Zhang, W. Peng, F. Xiuzhu, C. Tai-Shung, Sustainable water recovery from oily waste water via forward osmosis-membrane distillation (FO-MD), *Water Res.* 52 (2014) 112–121.
- [2] D. Abdessemed, G. Nezzal, R. Ben Aim, Coagulation-adsorption-ultrafiltration for wastewater treatment and reuse, *Desalination* 131 (2000) 307–314.
- [3] M. Abbasi, A. Salahi, M. Mirfendereski, T. Mohammadi, A. Pak, Dimensional analysis of permeation flux for microfiltration of oily wastewaters using mullite ceramic membranes, *Desalination* 252 (2010) 113–119.
- [4] W. Chen, Y. Su, L. Zheng, I. Wang, Z. Jiang, The improved oil/water separation performance of cellulose acetate-graft-polyacrylonitrile membranes, *J. Membr. Sci.* 337 (2009) 98–105.
- [5] F.-R. Ahmadun, A. Pendashteh, L.C. Abdullah, D.R.A. Biak, S.S. Madaeni, Z.Z. Abidin, Review of technologies for oil and gas produced water treatment, *J. Hazard. Mater.* 170 (2009) 530–551.

- [6] A.J. Burggraaf, L. Cot, *Fundamentals of Inorganic Membrane Science and Technology*, Elsevier Science, Amsterdam, 1996.
- [7] J. Cui, X. Zhang, H. Liu, S. Liu, K.L. Yeung, Preparation and application of zeolite/ceramic microfiltration membranes for treatment of oil contaminated water, *J. Membr. Sci.* 325 (2008) 420–426.
- [8] S.J. Maguire-Boyle, A.R. Barron, A new functionalization strategy for oil/water separation membranes, *J. Membr. Sci.* 382 (2011) 107–115.
- [9] C. Su, Y. Xu, W. Zhang, Y. Liu, J. Li, Porous ceramic membrane with superhydrophobic and superoleophilic surface for reclaiming oil from oily water, *Appl. Surf. Sci.* 258 (2012) 2319–2323.
- [10] M. Drobek, J. Motuzas, M.V. Loon, R.W.J. Dirrix, R.A. Terpstra, A. Julbe, Coupling microwave-assisted and classical heating methods for scaling-up MFI zeolite membrane synthesis, *J. Membr. Sci.* 401–402 (2012) 144–151.
- [11] H. Li, J. Wang, J. Xu, X. Meng, B. Xu, J. Yang, S. Li, J. Lu, Y. Zhang, X. He, D. Yin, Synthesis of zeolite NaA membranes with high performance and high reproducibility on coarse macroporous supports, *J. Membr. Sci.* 444 (2013) 513–522.
- [12] A.D.S. Barbosa, A.D.S. Barbosa, M.G.F. Rodrigues, Synthesis of MCM-22 zeolite membrane on a porous alumina support, *Mater. Sci. Forum* 805 (2014) 272–278.
- [13] R.C.N. Leite, B.V. Sousa, M.G.F. Rodrigues, Static synthesis and characterization of MCM-22 zeolite applied as additive in fluid catalytic cracking operations, *Braz. J. Petrol. Gas* 3 (2009) 75–82.
- [14] K. Tao, C. Kong, L. Chen, High performance ZIF-8 molecular sieve membrane on hollow ceramic fiber via crystallizing-rubbing seed deposition, *Chem. Eng. J.* 220 (2013) 1–5.
- [15] M.F. Mota, J.A. Silva, M.B. Queiroz, H.M. Laborde, M.G.F. Rodrigues, Organophilic clay for oil/water separation process by finite bath tests, *Braz. J. Petrol. Gas* 5 (2011) 97–107.
- [16] J. Yang, J.Y. Yang, Y. Zhou, F. Wei, W.G. Lin, J.H. Zhu, Hierarchical functionalized MCM-22 zeolite for trapping tobacco specific nitrosamines (TSNAs) in solution, *J. Hazard. Mater.* 179 (2010) 1031–1036.
- [17] A.S. Barbosa, A.S. Barbosa, M.G.F. Rodrigues, Synthesis of zeolite membranes through two distinct methods: Rubbing e dip coating, 11th International Conference on Catalysis in Membrane Reactors, Porto, July 7–11, 2013b.
- [18] A.S. Barbosa, A.S. Barbosa, M.G.F. Rodrigues, Synthesis of MCM-22 zeolite membrane on a porous alumina support, IPMM 2012, 7th International Conference on Intelligent Processing and Manufacturing of Materials, September, 2–3, 2012, Foz do Iguaçu, Brazil.
- [19] F.A. Silva, H.L. Lira, Preparation and characterization of cordierite ceramic membranes, *Cerâmica* 52 (2006) 276–282.
- [20] R.C.O. Lima, H.L. Lira, G.A. Neves, M.C. Silva, C.D. Silva, Aproveitamento do resíduo de serragem de granito para fabricação de membranas cerâmicas de baixo custo, *Rev. Eletrônica Mater. Processos* 63 (2011) 163–169.
- [21] Y.P. Pan, W. Wang, T.H. Wang, P.J. Yão, Fabrication of carbon membrane and microfiltration of oil-in-water emulsion: An investigation on fouling mechanisms, *Sep. Purif. Technol.* 57 (2007) 388–393.
- [22] R.R. Bhave, H.L. Fleming, Removal of oily contaminant in waste water with microporous alumina membranes, *AIChE Symp. Ser.* 84 (1988) 19–27.
- [23] Conama Resolução nº 392, de 08 de agosto de 2007 que dispõe sobre o descarte contínuo de água de processo ou de produção em plataformas marítimas de petróleo e gás natural e dá outras providências (CONAMA Resolution no 392, of August 8, 2007 boasts about contínuo disposal of process water or production in maritime oil platforms and natural gas and other providences). Publicada no DOU de 9 de agosto de 2007 (Published in Gazette of August 9, 2007).